Predicting Nerve Guidance Conduit Performance for Peripheral Nerve Regeneration using Bootstrap Aggregated Neural Networks

William Koch, Yan Meng, Munish Shah, Wei Chang, and Xiaojun Yu

Abstract— **The inability to identify the optimal construction of a nerve guidance conduit (NGC) for peripheral nerve regeneration is a challenge in the field of tissue engineering. This is attributed to the vast number of parameters that can be combined in varying quantities. A pre-existing normalization standard is applied in this paper which uses a calculated ratio of gap length divided by the graft′s critical axon elongation denoted as L/L_c. This allows for a direct comparison of the nerve regenerative activity, a measure of performance, of any NGC across an array of gap lengths relative to a standard nerve conduit. Data was extracted from a total of 28 scientific publications that compared the nerve regenerative activity of experimental NGCs relative to standard NGCs. Of the extracted data, 40 parameters were identified that impacted the performance of the experimental conduits. We demonstrate how bootstrap aggregated neural networks provides substantial increases in accuracy in predicting the performance of a NGC over a single neural network and previous prediction attempts by the SWarm Intelligence based Reinforcement Learning (SWIRL) system. The improved accuracy will provide for a better understanding and insight for theorizing successful strategies for NGC development.**

I. Introduction

THE peripheral nervous system (PNS) is composed of the nerves and ganglia outside of the brain and spinal cord that functions to connect the central nervous system to the limbs and organs. A peripheral nerve injury is damage to the nerves and/or its surrounding tissue. Peripheral nerve injuries caused by trauma or iatrogenic injury are a serious clinical problem [1]. Depending on the severity of the damage surgical intervention may be required given the limited regenerative ability of the peripheral nervous system. Over 50,000 repair procedures were performed in 1995 in the United States alone [2]. The surgical methods available to treat peripheral nerve injury are direct suturing of the proximal and distal nerve stumps if the nerve gap is $<$ 4mm and the application of a nerve autograft if the nerve gap $>$ 4mm, which is the gold standard. A nerve autograft is a segment of the nerve obtained from the patient and grafted between the proximal and distal nerve stumps to restore functionality [3]. The limited availability of autografts as well as a second surgical site(donor site) may lead to loss of function at the donor site which begs the progress for the alternative; guidance channels which are tubular nerve guidance conduits (NGCs) used to bridge the proximal and distal nerve stumps of the peripheral nerve gap [4]. Numerous conduits have been tested but only a few so far have received FDA approval, Neurotube®, NeuraGen®, Neuroflex™, NeuroMatrix™, AxoGuard™, and Neurolac® [5]. Due to the vast variety of experimental practices used by researchers for in vivo procedures an effective comparison between the nerve regenerative activities among the NGCs is required. A rat sciatic nerve model is generally used as a standard animal specie and anatomical site [6]. The remaining factors such as recovery time, gap length, conduit type, and additional enhancements to the conduit must be accounted for in order to make a valid comparison of conduit effectiveness. The need for standardization is critical to make a valid comparison of nerve regenerative activity between NGCs.

This paper is outlined as follow. In Section II the normalization standard that served as the basis of the model target output is discussed along with the input parameters. In Section III we give an overview of bootstrapping. We elaborate on how bootstrapping can be applied in Section IV to provide for increased accuracy in models to form aggregated predictors. In Section V we describe the implementation of the bootstrap aggregated (bagging) neural network (NN). Section VI examines the performance difference between training with backpropagation and Particle Swarm Optimization (PSO), the optimal number of neural networks used in an ensemble and benchmarking between a single NN and a previous attempt of estimating NGC performance by the SWarm Intelligence based Reinforcement Learning (SWIRL) model. Section VII summarized experimental results and future work.

II. Data Preparation

Due to the lack of a standard protocol, scientific journals are the domain by which researchers share their experiences and protocols to drive forward the development of effective and successful conduits. A novel method of normalization for comparison of the regenerative activity of conduits has been proposed by [7] calculated as the ratio of gap length divided by the grafts critical axon elongation denoted as L/Lc. This is based on the frequency of innervation, %N, which is widely used in experimental procedures of the rat sciatic nerve model and the normalization procedure is based on the assumption that a small increase in gap length bridged by a silicon tube will have a sharp drop in %N. The L_c is based on %N and denoted as the critical axon elongation at which the %N drops below 50%. An S shaped curve

W. Koch and Y. Meng are with the Department of Electrical and Computer Engineering, Stevens Institute of Technology, Hoboken, NJ 07030, USA. (email: {wkoch, yan.meng}@stevens.edu).

M. Shah, W. Chang and X. Yu are with the Department of Chemistry, Chemical Biology, and Biomedical Engineering, Stevens Institute of Technology, Hoboken, NJ 07030, USA. (email: {mshah37, wchang1, xiaojun.yu}@stevens.edu).

978-1-4673-6129-3/13/$31.00 ©2013 IEEE

for the rat sciatic nerve model, which plots the %N with respect to various gap lengths, was developed based on the data collected for an array of gap lengths bridged using an unfilled silicone tube implanted in the sciatic nerve of rats by [7]. The L_c value is estimated as a linear shift on the x-axis with respect to the value of %N and the gap length. The gap length divided by the critical axon elongation yields a dimensionless measure of the regenerative activity of a NGC. From an array of scientific publications we found 28 articles [3, 8–34] that matched the criteria for the L/L_c: reporting the gap length of study, a comparison of an experimental conduit against a standard conduit, and detailing the protocol and materials applied to the experiment. This yielded 138 cases, each detailing a particular conduit and the protocol for developing the conduit. In addition the measure of regeneration derived using the L/L_c method was reported. Table I illustrates the parameters used in the development and enhancement of NGCs based on their application. From the 138 cases, 40 parameters were identified to be significant in NGC development and used as the predictors input. These parameters include the conduit length along with parameters defined in Table I. Not all categories were used by every case, and some conduits used a combination of parameters. ΔL, computed by (1), is the difference between the regenerative activity of the experimental conduit (exp) and the standard conduit (std). This is a measure of the regenerative activity of the experimental conduit compared to the standard conduit.

$$\Delta L = L/L_c^{exp} - L/L_c^{std} \tag{1}$$

The value ΔL is our measure of performance in this paper and an output of our predictor. Additionally, we use time (in weeks) as an output to estimate the performance of the nerve guidance conduit. Time is an essential indicator of nerve regeneration and has an impact on the outcome of the treatment applied for nerve injury. Ideally with more time nerve regeneration can improve, as such better results can be observed. Providing time as an output allows for the user to be able to expect the ΔL to occur in the given time frame.

TABLE I

THE INPUT PARAMETERS CATEGORIZED BASED ON THEIR APPLICATION TO THE DEVELOPMENT AND ENHANCEMENT OF NGCS

Category	Model Input Parameters
Materials Processing	Phase Separation, Hydrogels, Electrospinning, Reverse Plating, Micropatterning, Liquid Filled
Structure	Fiber-Aligned, Fiber-Random, Gel, Permeable, Solid Tube (Impermeable), Microsphere, Porous, Internal Diameter, Wall Thickness, Lumen
Materials	Collagen, Ethyl Vinyl Acetate, Polycaprolactone, Poly Lactide, Poly Glycolic Acid, Poly Lactide Co Glycotide, Chitosan, Poly Phosphazene, Poly Pyrrole, Poly Sulfone, Silicone
Form	Hydrogel, Liquid, Gel, Matrix, Fiber-Aligned, Fiber-Random, Microsphere, Solid
Growth Factors	NGF, NT3, BDNF, CNTF, GDNF, PDGF, VEGF, FGF, Denatured FGF, IGF, Laminin, Fibronectin, Schwann Cells, Bone Marrow Stromal Cells, Neural Crest Stem Cells, Fibroblasts, Alpha1-GP
Growth Factor Arrangements	Gradients or Anisotropic, Isotropic

III. BOOTSTRAPPING

Bootstrapping [35] is a re-sampling technique based on the idea that the true probability distribution of a population can be modelled by re-sampling an empirical distribution obtained from the original observed data set.

Reference [36] claims that bootstrapping can be helpful when:

- the theoretical distribution or a statistic is complicated or unknown
- the sample sample size is insufficient for straightforward statistical inference
- power calculations have to be performed, and a small pilot sample is available

There are two bootstrap sampling approaches for regression, sampling by pairs or residuals [37]. If the observed training data set is of size n, the bootstrap pairs approach follows that a collection of n examples, $\{(x_1, y_1), (x_2, y_2), ..., (x_n, y_n)\}$, is drawn with replacement from the empirical distribution to form a single bootstrap sample. Here (x_i, y_i) is a single sample where x_i is the input vector of sample i and y_i is the corresponding output vector. To distinguish between multiple bootstrap samples the notation $\left\{(x_1^{*b}, y_1^{*b}), (x_2^{*b}, y_2^{*b}), ..., (x_n^{*b}, y_n^{*b})\right\}$ is used for each b bootstrap sample, where the asterisk $(*)$ indicates the sample is a bootstrap sample. The residual approach samples the model residuals, $\epsilon_j = y_j - \hat{y}_j$, with replacement, where the difference is taken between the observed value y_j and the estimated value $\hat{y}_j$. Each randomly sampled residual is added to the estimated output $\hat{y}_i$ to form a bootstrap sample $\left\{(x_1, \hat{y_1} + \epsilon_1^{*b}), (x_2, \hat{y_2} + \epsilon_2^{*b}), ..., (x_n, \hat{y_n} + \epsilon_n^{*b})\right\}$. ϵ_j^{*b} is the jth randomly sampled residual where this set is for the bth bootstrap sample, again denoted by the asterisk. x_i is the corresponding input pair for the estimated output $\hat{y}_i$.

The primary difference between the two methods as described by [38] is that the pairs approach provides an unconditional bootstrap distribution while the residual approach provides a conditional bootstrap distribution. The conditional factor retains to the observed data set. The re-samples of the training observations in the pairs approach allow for an underlying distribution of the population to be found rather than the distribution found strictly from the training observations used by the residuals approach. One must select the appropriate method pertaining to their target objective.

IV. BOOTSTRAP AGGREGATING PREDICTORS

Bootstrap aggregating predictors is a method in which an ensemble of predictors are trained on unique bootstrap samples and combine to form an aggregated predictor [39]. It has been demonstrated in multiple examples [39–41] that an aggregation of predictors can provide for increase

in accuracy, improved generalization and robustness when compared to a single predictor.

Bagged predictors are more accurate than single predictors based on the assumption that an ensemble of predictors will cause less error than a single predictor. There is less chance of multiple predictors causing more error than a single predictor. Typically a single predictor's estimate is more uncertain than a bagged predictor as it may have non-optimal initial construction or suffer from over-fitting based on the partitioning of the data set [37, 40].

A bagged predictor is constructed by creating B predictors. B bootstrap samples are then obtained from the original training data set. The bth predictor is trained on the bth bootstrap sample. Result $\hat{y}$ from a bagged predictor is found for regression tasks by computing the mean (2) of each individual predictors outputs $\hat{y}^b$ while in classification a vote is taken.

$$\hat{y} = \frac{1}{B}\sum_{b=1}^{B}\hat{y}^b \tag{2}$$

B are the number of predictors, whereas $\hat{y}^b$ is the output from each predictor in the ensemble

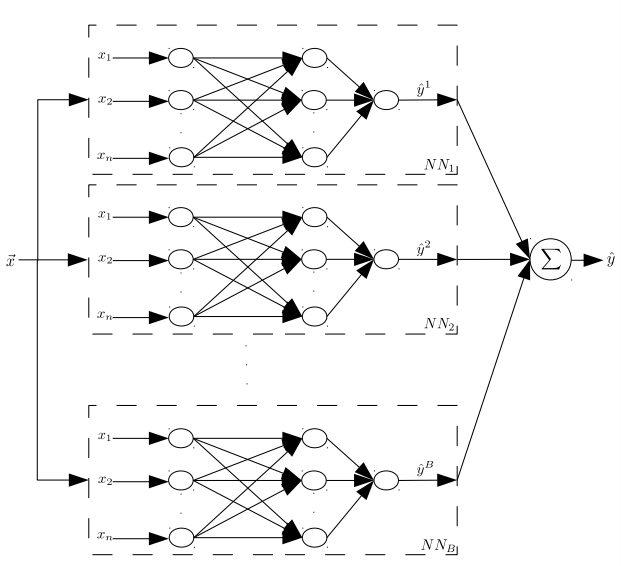

Fig. 1. Bagged neural network.

V. Experimental Setup

To test the estimation of NGC performance using a bagged predictor, a single feedforward neural network (FFNN) is used as the control. A bagged predictor was created using a FFNN as the predictor (Fig.1). Since the bagged NN is a collection of FFNN this will give us true indication of performance. Both networks are to be trained with backpropagation and Particle Swarm Optimization (PSO) [42].

Experimentation was conducted to find the optimal network topology for each training strategy. According to [43], one hidden layer should be sufficient for modelling most scenarios however two may be needed for more complex situations. One of many rules of thumb for determining hidden node count is to have the count between the number of input nodes and number of output nodes. Based on this information we investigate network topologies of one and two hidden layers. For networks trained with backpropagation, we range the hidden nodes for each layer between 1 and 40 nodes and when trained with PSO we range the hidden nodes for each layer between 1 and 10 nodes. We limit the number of hidden nodes to 10 when trained with PSO based on previous experience of not seeing added benefit above this number that come with additional computational expense. Our results displayed in Fig. 2 conclude that the optimal topology for a network trained with backpropagation for this data set is a network with two hidden layers, the first with 20 hidden nodes and the second with 1 hidden node. The results for training with PSO displayed in Fig. 3 conclude a single hidden layer with 5 nodes is optimal. From this point forward experimentation using FFNNs and bagged NNs trained with backpropagation are implemented with a network topology of 40-20-1-2 and when trained with PSO are implemented with a topology of 40-5-2. The input units were constructed with linear transfer functions while hyperbolic tangent transfer functions were used for the hidden and output units. Bias units are used for hidden and output layers.

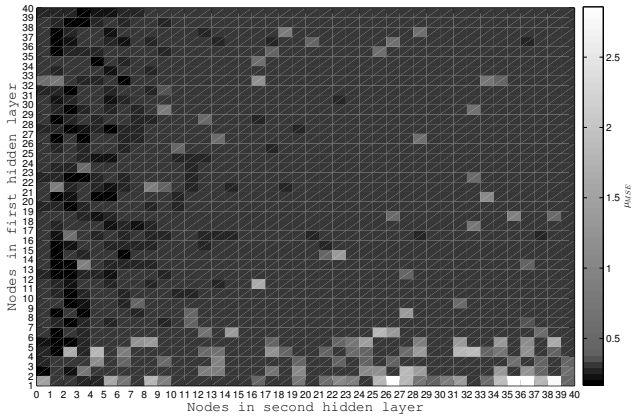

Fig. 2. Color map displaying network topology performances when trained with backpropagation. The color bar indicates mean MSE,μ_{MSE}, of 50 trials conducted for each topology. 50 instances of the data set are randomly partitioned at the beginning of the experiment so each topology is trained and tested on each of the 50 instances to ensure results reflect topology performance. Darker represents lower error. The lowest error is acheived with 20 nodes in the first layer and one node in the second layer.

The data set contained 110 observed cases after pre-processing and partitioned randomly for each experimental trial instance to produce 80% training and 20% testing cases to ensure an unbiased training and testing sample. The range of B has been defined by [44] to between 25-200 to which the experiments conducted shall abide by. Referring back to Section. III, bootstrap pairs approach is selected for sampling because we are concerned with an unconditional distribution and do not want to be limited to the collected training

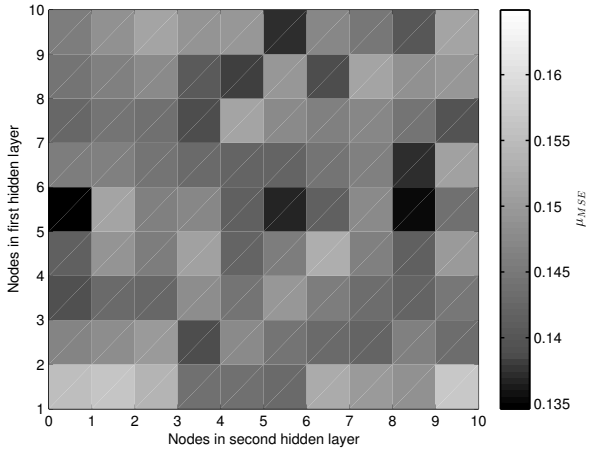

Fig. 3. Color map displaying network topology performances when trained with PSO. The color bar indicates mean MSE,μ_{MSE}, of the 50 trials conducted for each topology. 50 instances of the data set are randomly partitioned at the beginning of the experiment so each topology is trained and tested on each of the 50 instances to ensure results reflect topology performance. Darker represents lower error. The lowest error is acheived with 5 nodes in the first layer and zero nodes in the second layer (i.e., the second layer is not used).

observations. All model implementation were written in Java and executed on a 64-bit Intel® Core™i7 @ 2.20GHz processor with 8GB of RAM.

Four experiments are conducted. The first determines the optimal number of networks in an ensemble when trained with backpropagation. The second experiment benchmarks the result found compared to a FFNN trained with back-propagation and the SWIRL model. The third experiment investigates the optimal number of networks in an ensemble when trained with PSO, and the last experiment performs another benchmark using the bagged NN with optimal size, FFNN trained with PSO and SWIRL.

In the 2nd and 4th experiments, as previously mentioned, the FFNN and bagged NN are compared to SWIRL, SWarm Intelligence based Reinforcement Learning [45] which as far as we know is the only other model that has been used to predict NGC performance. SWIRL is a school system model where Ant Colony Optimization (ACO) [46] acts as the administrator, PSO represents the teachers and each NN in an ensemble acts as a student. ACO essentially models the navigation behaviour of ants and is applied in this context to find the optimal NN topology and PSO is used to train each of the NN students. Once SWIRL finds the optimal NN it can be used for testing. The SWIRL model configuration is unchanged through the experiments. It is configured with 100 students, PSO parameters of cognitive and social learning rates set to 2.0 and inertia weight set to 0.8, and ACO parameters of pheromone influence factor $\alpha = 2.0$, desirability influence factor $\beta = 1.0$, and pheromone persistence $\rho = 0.5$. Network topology was defined as 40-H-1 where H ranged from 3 to 15 hidden units. Linear transfer functions were used for input units and hyperbolic tangent transfer functions were used for hidden and output units.

VI. Experimental Results

The first experiment is conducted to find the optimal size of the ensemble. At the beginning of the experiment, 10 instances of the data set are formed where each instance is a random partition of training and testing data. Each of the 10 constructed instances are then used to train and test every ensemble size to ensure the size is the only varying change. Backpropagation is chosen as a benchmark since it is the most commonly used training algorithm. The learning rate was set to 0.01 and the momentum to 0.95. The results are show in Fig.4. Network sizes B were chosen between 20 to 200, in increments of 20 represented on the x-axis. The y-axis in the top subgraph, μ_{MSE}, is the averaged Mean Square Error (MSE) (3) of the 10 trials where n is the number of testing cases, $\hat{y}_i$ is the output of the predictor and y_i is the true output value.

$$MSE = \frac{1}{n}\sum_{i=1}^{n}(\hat{y}_i - y_i)^2 \tag{3}$$

The y-axis in the bottom subgraph, σ^2_{MSE}, is the variance between the MSE of the 10 trials.

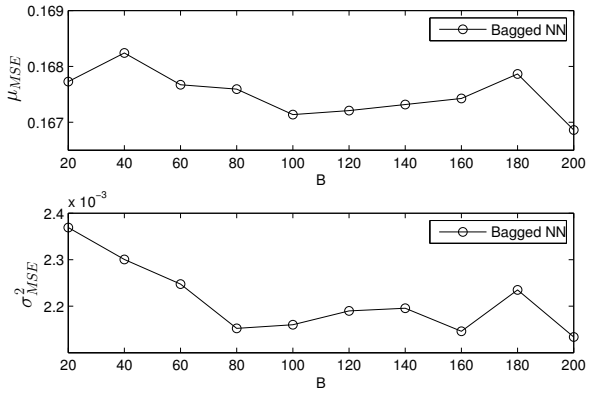

Fig. 4. Testing the optimal number of networks in an ensemble when trained with backpropagation. The top subgraph displays the mean MSE from 10 trials and the bottom subgraph displays the varaince between the trials.

Results indicate that the network is most accurate at $B = 200$ and its variance between estimates is also the lowest. The average time to train and test the ensemble of this size took 1.41 minutes. To gauge the performance of the bagged NN we conduct the second experiment to compare the results to a FFNN and the SWIRL model. The FFNN and SWIRL models were trained and tested in parallel during the experiment thus the results shown in Fig. 5 are based on all three models being trained and tested on the same data. A summary of the of the overall μ_{MSE} and σ^2_{MSE} results can be seen in Table II. All three models perform similarly. The SWIRL model performs slightly better however the variance has almost doubled.

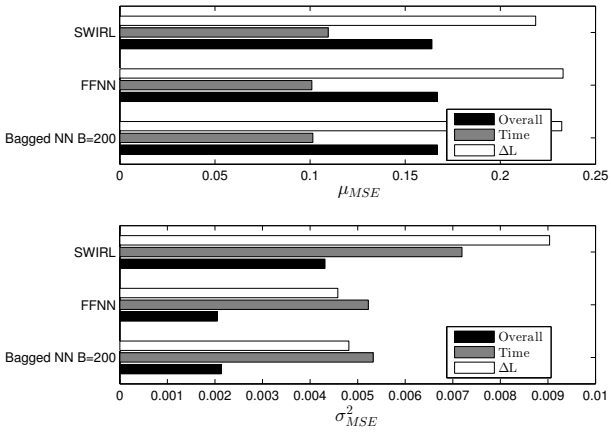

Fig. 5. Comparison between models with FFNN and Bagged NN trained with backpropagation. The top subgraph displays the mean MSE from 10 trials and the bottom subgraph displays the varaince between the trials. The black bar indicates the over all output eror while the gray and white bars indicate the error level for each specific model output.

TABLE II
SUMMARY OF BENCHMARK RESULTS WHEN FFNN AND BAGGED NN ARE TRAINED WITH BACKPROPAGATION

Model	μ_{MSE}	σ^2_{MSE}
SWIRL	0.1640330886	0.0043129584
FFNN	0.166960802	0.0020485363
Bagged NN B=200	0.1668624806	0.0021338728

The third experiment conducted to find the optimal size of the ensemble when trained using PSO. PSO is a population based optimization algorithm in which particles evolve in search-space to find solutions to a problem. PSO was configured to have an initial population of 40, cognitive and social learning rates set to 2.0 and inertia weight set to 0.4. Max velocity was limited to 2.0. Network sizes B were chosen from 20 to 200, in increments of 20 as in the previous experiment. Construction of the data sets for the 10 trial instances was also performed the same as the last experiment. Fig. 6 indicates that a bagged NN of $B = 180$ trained with PSO is optimal. The average time to train and test the ensemble of this size took 20.07 minutes.

Finally the fourth experiment is performed to compare the optimal ensemble size to the other models which is depicted in Fig. 7. At first glance we see the increase in accuracy when the FFNN and bagged NN are trained with PSO compared to training with backpropagation. The variance between trials has also dropped dramatically. The bagged NN with optimal network size $B = 180$ out performs all other models in both accuracy and consistency, as reflected by the variance.

A detailed comparison of the overall μ_{MSE} and σ^2_{MSE} are displayed in Table III. Results show that the bagged NN reduced the error from the SWIRL model by 40.48% and had an error reduction of 22.21% compared to the FFNN.

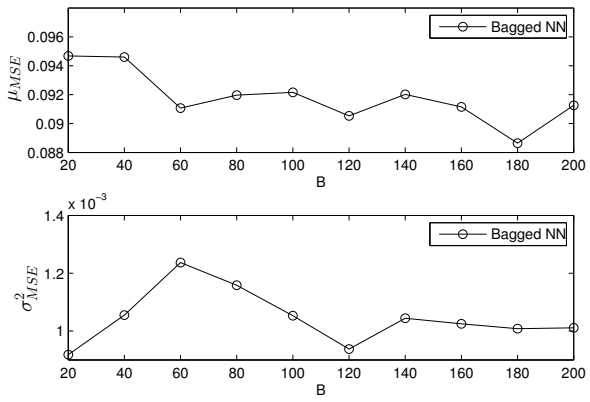

Fig. 6. Testing the optimal number of networks in an ensemble when trained with PSO. Top subgraph displays the mean MSE from 10 trials and the bottom subgraph displays the varaince between the trials.

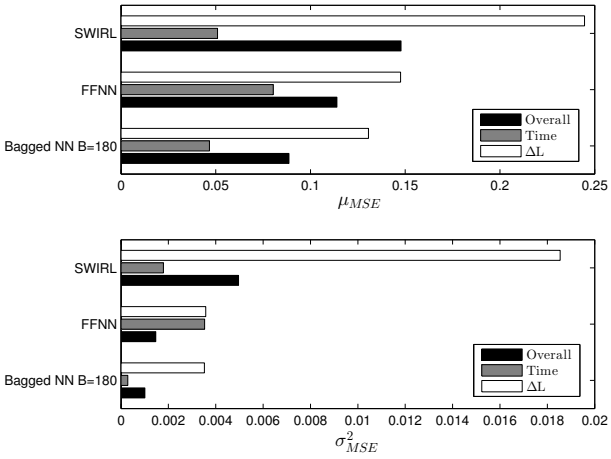

Fig. 7. Comparison between models with FFNN and Bagged NN trained with PSO. The top subgraph displays the mean MSE from 10 trials and the bottom subgraph displays the varaince between the trials. The black bar indicates the over all output eror while the gray and white bars indicate the error level for each specific model output.

VII. CONCLUSIONS

A bagged NN is a straight forward way to greatly increase prediction accuracy over a single NN as demonstrated in predicting the performance of a NGC. The major drawback to this method is the computational expense which was quite evident with the larger size ensembles. Training with PSO had the longest execution time however this may be reduced with further tuning of the PSO parameters. Furthermore PSO training did produce the greatest decrease in the error which may out weigh the computational expense. In any case both bagged NN training procedures out preformed the single FFNN. We have also demonstrated that using a bagged NN trained with PSO out performs the previous attempt of estimating NGC performance by the SWarm Intelligence based Reinforcement Learning (SWIRL) model by a 40.48%

TABLE III
SUMMARY OF BENCHMARK RESULTS WHEN FFNN AND BAGGED NN ARE TRAINED WITH PSO

Model	μ_{MSE}	σ^2_{MSE}
SWIRL	0.1489327521	0.003882092
FFNN	0.1139504194	0.0014665992
Bagged NN B=180	0.088646432	0.0010082951

decrease in error. The primary difference between the FFNN trained with PSO and SWIRL is the dynamic topology SWIRLs implements. The FFNN trained with PSO proves more accurate in the forth experiment thus suggesting that the stochastic nature of PSO misleads SWIRL to choosing an un-optimal topology causing poor performance.

The main challenge with predicting the performance of a NGC is the limited number of experimental cases, as single experiments may take as long as 60 weeks to complete [26]. This in conjunction with large number of model parameters causes the predictors to suffer from Hughs Effect [47] in which the prediction accuracy decreases as the dimensionality of the problem increases. The high dimensionality also causes the model to be subjected to overfitting when data set size is small. Fortunately there has been knowledge rules extracted from these experiments. In future work we plan to take advantage of this additional knowledge to make more accurate predictions of NGC performance. Bootstrapping has the added benefit of being able to construct confidence and prediction intervals [37, 40, 44, 48, 49]. We intend to leverage the use of prediction intervals to act as an indicator of the level the bagged NN can be trusted. Depending on the trust level, the model will determine the degree of influence the additional domain knowledge will have on the predicted output thus further increasing accuracy. Additional knowledge can also be used to generate virtual training examples [50]. Virtual examples create new training examples from the existing data set by transforming the original data based on domain knowledge. These addition virtual training examples can aid in the generalization of the model and decrease the likelihood of overfitting. Bootstrap aggregated neural networks used to estimate the performance of a nerve guidance conduit has been shown to enhance the progress towards developing an optimal conduit to restore function from a peripheral nerve injury.

ACKNOWLEDGMENT

This work was supported by NIH-R15 NS074404.

REFERENCES

[1] W. W. Campbell, "Evaluation of peripheral nerve injury," *European Journal of Pain Supplements*, vol. 3, no. S2, pp. 37–40, 2009.

[2] R. V. Bellamkonda, "Peripheral nerve regeneration: an opinion on channels, scaffolds and anisotropy," *Biomaterials*, vol. 27, no. 19, pp. 3515–3518, 2006.

[3] X. Yu and R. V. Bellamkonda, "Tissue-engineered scaffolds are effective alternatives to autografts for bridging peripheral nerve gaps," *Tissue engineering*, vol. 9, no. 3, pp. 421–430, 2003.

[4] S. E. Mackinnon, A. L. Dellon *et al.*, "Clinical nerve reconstruction with a bioabsorbable polyglycolic acid tube." *Plastic and reconstructive surgery*, vol. 85, no. 3, p. 419, 1990.

[5] S. Kehoe, X. Zhang, and D. Boyd, "Fda approved guidance conduits and wraps for peripheral nerve injury: A review of materials and efficacy," *Injury*, vol. 43, no. 5, pp. 553–572, 2012.

[6] I. V. Yannas and B. J. Hill, "Selection of biomaterials for peripheral nerve regeneration using data from the nerve chamber model," *Biomaterials*, vol. 25, no. 9, pp. 1593–1600, 2004.

[7] M. Zhang and I. V. Yannas, "Peripheral nerve regeneration," *Regenerative Medicine II*, pp. 130–130, 2005.

[8] H.-Y. Chiang, H.-F. Chien, H.-H. Shen, J.-D. Yang, Y.-H. Chen, J.-H. Chen, and S.-T. Hsieh, "Reinnervation of muscular targets by nerve regeneration through guidance conduits," *Journal of Neuropathology & Experimental Neurology*, vol. 64, no. 7, pp. 576–587, 2005.

[9] T. Bini, S. Gao, S. Wang, A. Lim, L. B. Hai, S. Ramakrishna *et al.*, "Electrospun poly (l-lactide-co-glycolide) biodegradable polymer nanofibre tubes for peripheral nerve regeneration," *Nanotechnology*, vol. 15, no. 11, p. 1459, 2004.

[10] K. Ohbayashi, H. K. Inoue, A. Awaya, S. Kobayashi, H. Kohga, M. Nakamura, and C. Ohye, "Peripheral nerve regeneration in a silicone tube: effect of collagen sponge prosthesis, laminin, and pyrimidine compound administration." *Neurologia medico-chirurgica*, vol. 36, no. 7, p. 428, 1996.

[11] M. H. Spilker, "Peripheral nerve regeneration through tubular devices: a comparison of assays of device effectiveness," Ph.D. dissertation, Massachusetts Institute of Technology, 2000.

[12] L. Yao, G. C. de Ruiter, H. Wang, A. M. Knight, R. J. Spinner, M. J. Yaszemski, A. J. Windebank, and A. Pandit, "Controlling dispersion of axonal regeneration using a multichannel collagen nerve conduit," *Biomaterials*, vol. 31, no. 22, pp. 5789–5797, 2010.

[13] R. Ikeguchi, R. Kakinoki, T. Matsumoto, T. Yamakawa, K. Nakayama, Y. Morimoto, H. Tsuji, J. Ishikawa, and T. Nakamura, "Basic fibroblast growth factor promotes nerve regeneration in a c¡ sup¿-¡/sup¿-ion-implanted silicon chamber," *Brain research*, vol. 1090, no. 1, pp. 51–57, 2006.

[14] M. D. Wood, A. M. Moore, D. A. Hunter, S. Tuffaha, G. H. Borschel, S. E. Mackinnon, and S. E. Sakiyama-Elbert, "Affinity-based release of glial-derived neurotrophic factor from fibrin matrices enhances sciatic nerve regeneration," *Acta biomaterialia*, vol. 5, no. 4, pp. 959–968, 2009.

[15] W. F. Den Dunnen, B. van der Lei, J. M. Schakenraad, E. H. Blaauw, I. Stokroos, A. J. Pennings, and P. H. Robinson, "Long-term evaluation of nerve regeneration in a biodegradable nerve guide," *Microsurgery*, vol. 14, no. 8, pp. 508–515, 2005.

[16] C.-B. Jenq and R. Coggeshall, "Numbers of regenerating axons in parent and tributary peripheral nerves in the rat," *Brain research*, vol. 326, no. 1, pp. 27–40, 1985.

[17] P. Aebischer, A. Salessiotis, and S. Winn, "Basic fibroblast growth factor released from synthetic guidance channels facilitates peripheral nerve regeneration across long nerve gaps," *Journal of neuroscience research*, vol. 23, no. 3, pp. 282–289, 2004.

[18] A. C. Lee, V. M. Yu, J. B. Lowe, M. J. Brenner, D. A. Hunter, S. E. Mackinnon, and S. E. Sakiyama-Elbert, "Controlled release of nerve growth factor enhances sciatic nerve regeneration," *Experimental neurology*, vol. 184, no. 1, pp. 295–303, 2003.

[19] C.-J. Chen, Y.-C. Ou, S.-L. Liao, W.-Y. Chen, S.-Y. Chen, C.-W. Wu, C.-C. Wang, W.-Y. Wang, Y.-S. Huang, and S.-H. Hsu, "Transplantation of bone marrow stromal cells for peripheral nerve repair," *Experimental neurology*, vol. 204, no. 1, pp. 443–453, 2007.

[20] A. Ansselin, T. Fink, and D. Davey, "Peripheral nerve regeneration through nerve guides seeded with adult schwann cells," *Neuropathology and applied neurobiology*, vol. 23, no. 5, pp. 387–398, 1997.

[21] G. Lundborg, L. Dahlin, D. Dohi, M. Kanje, and N. Terada, "A new type of bioartificial nerve graft for bridging extended defects in nerves," *The Journal of Hand Surgery: British & European Volume*, vol. 22, no. 3, pp. 299–303, 1997.

[22] L. J. Chamberlain, I. V. Yannas, H.-P. Hsu, and M. Spector, "Connective tissue response to tubular implants for peripheral nerve regeneration: the role of myofibroblasts," *The Journal of comparative neurology*, vol. 417, no. 4, pp. 415–430, 2000.

[23] X. Xu, H. Yu, S. Gao, H.-Q. Mao, K. W. Leong, and S. Wang, "Polyphosphoester microspheres for sustained release of biologically active nerve growth factor," *Biomaterials*, vol. 23, no. 17, pp. 3765–3772, 2002.

[24] P. M. George, R. Saigal, M. W. Lawlor, M. J. Moore, D. A. LaVan, R. P. Marini, M. Selig, M. Makhni, J. A. Burdick, R. Langer *et al.*, "Three-dimensional conductive constructs for nerve regeneration," *Journal of Biomedical Materials Research Part A*, vol. 91, no. 2, pp. 519–527, 2009.

[25] G. R. Evans, K. Brandt, A. D. Niederbichler, P. Chauvin, S. Hermann, M. Bogle, L. Otta, B. Wang, and C. W. Patrick, "Clinical long-term in vivo evaluation of poly (l-lactic acid) porous conduits for peripheral nerve regeneration," *Journal of Biomaterials Science, Polymer Edition*, vol. 11, no. 8, pp. 869–878, 2000.

[26] L. Chamberlain, I. Yannas, H. Hsu, G. Strichartz, and M. Spector, "Collagen-gag substrate enhances the quality of nerve regeneration through collagen tubes up to level of autograft," *Experimental neurology*, vol. 154, no. 2, pp. 315–329, 1998.

[27] C.-B. Jenq and R. E. Coggeshall, "Permeable tubes increase the length of the gap that regenerating axons can span," *Brain research*, vol. 408, no. 1, pp. 239–242, 1987.

[28] J. P. Hollowell, A. Villadiego, and K. M. Rich, "Sciatic nerve regeneration across gaps within silicone chambers: long-term effects of ngf and consideration of axonal branching," *Experimental neurology*, vol. 110, no. 1, pp. 45–51, 1990.

[29] M. C. Dodla and R. V. Bellamkonda, "Differences between the effect of anisotropic and isotropic laminin and nerve growth factor presenting scaffolds on nerve regeneration across long peripheral nerve gaps," *Biomaterials*, vol. 29, no. 1, pp. 33–46, 2008.

[30] L. R. Williams, N. Danielsen, H. Müller, and S. Varon, "Exogenous matrix precursors promote functional nerve regeneration across a 15-mm gap within a silicone chamber in the rat," *The Journal of comparative neurology*, vol. 264, no. 2, pp. 284–290, 2004.

[31] C.-B. Jenq, L. L. Jenq, and R. E. Coggeshall, "Nerve regeneration changes with filters of different pore size," *Experimental neurology*, vol. 97, no. 3, pp. 662–671, 1987.

[32] M. D. Wood, D. Hunter, S. E. Mackinnon, and S. E. Sakiyama-Elbert, "Heparin-binding-affinity-based delivery systems releasing nerve growth factor enhance sciatic nerve regeneration," *Journal of Biomaterials Science, Polymer Edition*, vol. 21, no. 6-7, pp. 771–787, 2010.

[33] S.-h. Hsu, C.-H. Su, and I.-M. Chiu, "A novel approach to align adult neural stem cells on micropatterned conduits for peripheral nerve regeneration: a feasibility study," *Artificial Organs*, vol. 33, no. 1, pp. 26–35, 2009.

[34] R. de Boer, A. M. Knight, A. Borntraeger, M.-N. Hébert-Blouin, R. J. Spinner, M. J. Malessy, M. J. Yaszemski, and A. J. Windebank, "Rat sciatic nerve repair with a poly-lactic-co-glycolic acid scaffold and nerve growth factor releasing microspheres," *Microsurgery*, vol. 31, no. 4, pp. 293–302, 2011.

[35] B. Efron and R. J. Tibshirani, *An introduction to the bootstrap*. Chapman & Hall/CRC, 1994, vol. 57.

[36] H. J. Ader, G. J. Mellenbergh, and D. J. Hand, *Advising on Research Methods: a consultant companion*. Johannes van Kessel Publ., 2008.

[37] R. Tibshirani, "A comparison of some error estimates for neural network models," *Neural Computation*, pp. 1–15, 1996.

[38] W. G. Baxt and H. White, "Bootstrapping confidence intervals for clinical input variable effects in a network trained to identify the presence of acute myocardial infarction," *Neural Computation*, vol. 7, no. 3, pp. 624–638, 1995.

[39] L. Breiman, "Bagging predictors," *Machine Learning*, vol. 24, no. 2, pp. 123–140, Aug. 1996.

[40] J. Zhang, "Developing robust non-linear models through bootstrap aggregated neural networks," *Neurocomputing*, vol. 25, no. 1-3, pp. 93–113, Apr. 1999.

[41] S. Hashem, B. Schmeiser, and Y. Yih, "Optimal linear combinations of neural networks: an overview," in *Neural Networks, 1994. IEEE World Congress on Computational Intelligence., 1994 IEEE International Conference on*, vol. 3. IEEE, 1994, pp. 1507–1512.

[42] J. Kennedy and R. Eberhart, "Particle swarm optimization," in *Neural Networks, 1995. Proceedings., IEEE International Conference on*, vol. 4. IEEE, 1995, pp. 1942–1948.

[43] J. Heaton, *Introduction to Neural Networks for Java (2nd Edition)*. Heaton Research, 2008.

[44] R. Dybowski and S. Roberts, "Confidence intervals and prediction intervals for feed-forward neural networks," *... applications of artificial neural networks*, 2001.

[45] M. Conforth, Y. Meng, C. Valmikinathan, and X. Yu, "Nerve graft selection for peripheral nerve regeneration using neural networks trained by a hybrid aco/pso method," in *Computational Intelligence in Bioinformatics and Computational Biology, 2009. CIBCB'09. IEEE Symposium on*. IEEE, 2009, pp. 208–214.

[46] M. Dorigo, V. Maniezzo, and A. Colorni, "Ant system: optimization by a colony of cooperating agents," *Systems, Man, and Cybernetics, Part B: Cybernetics, IEEE Transactions on*, vol. 26, no. 1, pp. 29–41, 1996.

[47] T. Oommen, D. Misra, and N. Twarakavi, "An objective analysis of support vector machine based classification for remote sensing," *Mathematical ...*, 2008.

[48] A. Khosravi, S. Nahavandi, D. Creighton, and A. F. Atiya, "Comprehensive review of neural network-based prediction intervals and new advances." *IEEE transactions on neural networks / a publication of the IEEE Neural Networks Council*, vol. 22, no. 9, pp. 1341–56, Sep. 2011.

[49] T. Heskes, "Practical confidence and prediction intervals," *Advances in neural information processing systems*, 1997.

[50] T. Yu, T. Jan, S. Simoff, and J. Debenham, "Incorporating prior domain knowledge into inductive machine learning," pp. 1–42, 2007.